Electronic Supplementary Material (ESI) for CrystEngComm.

Construction and theoretical study of a new Dy-β-diketone chain featuring slow magnetic relaxation

Yan-Chun Hui,[a] Yin-Shan Meng,[b] Zongsheng Li,[c] Qi Chen,[a] Hao-Ling Sun,[a]* Yi-Quan Zhang,[d] and Song Gao [b]*

[a] *Department of Chemistry and Beijing Key Laboratory of Energy Conversion and Storage Materials, Beijing Normal University, Beijing 100875, P. R. China. E-mail: haolingsun@bnu.edu.cn;*

[b] *Beijing National Laboratory for Molecular Sciences, State Key Laboratory of Rare Earth Materials Chemistry and Applications, College of Chemistry and Molecular Engineering, Peking University, Beijing 100871, China. E-mail: gaosong@pku.edu.cn;*

[c] *College of Safety and Environment Engineering, Capital University of Economics and Business, Beijing 100070, People's Republic of China*

[d] *Jiangsu Key Laboratory for NSLSCS, School of Physical Science and Technology, Nanjing Normal University, Nanjing 210023, P. R. China.*

Experimental section

Synthesis

All of the reagents used in the synthesis were obtained from commercial sources and without further purification.

1-phenyl-3-(4′-pyridyl)-propane-1,3-dione (HA): Acetophenone (24 mL, 208 mmol) was added to a solution of methyl isonicotinate (10 mL, 83 mmol) in tetrahydrofuran (220 mL) and stirred at room temperature for 10 min. Then, CH_3ONa (11.2 g, 208 mmol) was added to the solution during 30 min by small portions and the precipitation was gradually produced. The solution was further stirred at room temperature for 20 min and heated to reflux for 4 h. After resulting reaction mixture was cooled to room temperature, distilled water was added to the solution to dissolve the precipitate, and the solution was adjusted to pH = 5 by acetic acid. The aqueous solution was extracted with dichloromethane (3×30), the combined organic phase was dried over anhydrous Na_2SO_4 and the solvent was removed in vacuum. The resulting crude residue was purified by silica gel chromatography (10:1 v/v petroleum ether/EtOAc followed by 5:1 v/v of the same), to afford the desired product (HA, 10.3 g, 55.3 %) as a pale yellow solid. m/z $[M+H]^+$: 226.1; ^{1}H NMR(400 MHz, DMSO-d_6): δ 8.83-8.84 (d, 2H); 8.22 (d, 2H); 8.06-8.08 (d, 2H);7.73 (t, 1H);7.69-7.71 (t, 2H); 7.49 (s, 1H).

1-phenyl-3-(4′-pyridyl-N-oxide)-propane-1,3-dione (HL): To a solution of HA (10 g, 44 mmol) in dichloromethane (200 mL), m-chloroperoxybenzoic acid (m-CPBA, 18.9 g, 109.7 mmol, 85 %) was added during 30 min by small portions at 0 ℃. After the reaction mixture was stirred at room temperature for 6h, the precipitate was filtered and the filtrate was collected. Then the solvent was evaporated under reduced pressure. The final crude product was purified by silica gel chromatography (200:1 v/v dichloromethane/methanol followed by 60:1 v/v of the same), to give the desired product (HL, 6.0g, 56.1%) as a yellow solid. m/z $[M+H]^+$: 242.1; ^{1}H NMR(400 MHz, DMSO-*d6*): δ 8.39-8.41 (d, 2H); 8.16-8,21 (m, 4H); 7.67-7.69 (t,1H); 7.58-7.62 (t, 2H); 7.45 (s, 1H).

$[Dy(L)_3(H_2O)]\cdot0.5CH_3OH\cdot0.5H_2O$ (1): Compound **1** was prepared by the diffusion method in a test tube. There are three solutions, the bottom layer contains $Dy(NO_3)_3\cdot6H_2O$ (0.05mmol, 22.8mg) and CH_3COONa (0.15mmol, 12.3 mg) dissolved in 3 mL distilled water, the middle layer consists of 3 mL 1 : 1 water/ methanol mixture, and the top layer contains HL (0.15mmol, 36.2mg) dissolved in 3 mL methanol layered in a test tube. Then the components slowly diffused and obtained yellow needle single crystals of the compound **1** after two weeks, suitable for X-ray diffraction analysis, which were filtered off and air-dried. Yield: 19.3 mg (41.68%, based on the metal salt). Elemental analysis (%) calcd for $C_{42.5}H_{35}DyN_3O_{11}$: C, 55.11; H, 3.81; N, 4.54. Found (%): C, 55.50; H, 3.62; N, 4.57. Selected IR (KBr, cm^{-1}): 3091(br), 2369(w), 1599(s), 1570(m), 1518(s), 1464(s), 1418(s), 1219(m), 1177(m), 1026(w), 853(m), 766(m), 716(m), 667(w), 598(m), 519(m), 463(w).

X-ray crystallography and physical measurement

Intensity data for compound **1** were collected on a Bruker Smart Apex II CCD diffractometer with graphite-monochromated Mo Kα radiation (0.71073Å) at 293 K. The structures were solved by direct methods and refined with the full-matrix least-squares technique based on F^2 using the SHELXL program. All non-hydrogen atoms were refined anisotropically. Hydrogen atoms of the water molecules were located from the difference Fourier maps and refined with restraint of the O-H and H···H distances (0.96 and 1.52 Å, respectively). Other hydrogen atoms were placed at the calculation positions. The details of crystallographic data and selected bond parameters for compound **1** are listed in Table 1 and Table S1-S3, respectively. Power X-ray diffraction data for the sample was collected at room temperature on bulk samples with Cu Kα radiation (1.54059 Å).

Elemental analyses of carbon, hydrogen and nitrogen were carried out with an ElementarVario El analyzer. FTIR spectra were taken in the range of 4000 to 400 cm^{-1}on a Nicolet Magna 750 FT/IR spectrometer. Powder X-ray diffraction (XRD) analyses were performed on a Rigaku Dmax-2000 X-ray diffractometer with Cu Kα (λ=1.54059 Å) radiation. Variable-temperature magnetic susceptibility measurements of **1** were performed on an SQUID-VSM and PPMS magnetometer.

Computational details

For CASSCF calculations, the basis sets for all atoms are atomic natural orbitals from the MOLCAS ANO-RCC library: ANO-RCC-VTZP for Dy^{3+} ion; VTZ for close O and N; VDZ for distant atoms. The calculations employed the second order Douglas-Kroll-Hess Hamiltonian, where scalar relativistic contractions were taken into account in the basis set and the spin-orbit coupling was handled separately in the restricted active space state interaction (RASSI-SO) procedure. The active electrons in 7 active spaces include all *f* electrons (CAS(9 in 7)) in the CASSCF calculation. To exclude all the doubts we calculated all the roots in the active space. We have mixed the maximum number of spin-free state which was possible with our hardware (all from 21 sextets; 128 from 224 quadruplets; 130 from 490 doublets).

Table S1 Crystallographic Data and Structure Refinement for complex **1**

Formula	$C_{42.5}H_{35}DyN_3O_{11}$	μ (mm^{-1})	2.035
Mr	926.24	*F*(000)	3720
Crystal system	Orthorhombic	GOF	1.014
Space group	*P* bcn	Data collected	49156
a(Å)	35.022(3)	unique	8693
b(Å)	10.764(1)	R_{int}	0.0571
c(Å)	20.158(2)	*R*1 [$I > 2\sigma(I)$]	0.0301
V (Å^3)	7599.1(12)	*wR*2 [$I > 2\sigma(I)$]	0.0553
Z	8	*R*1 [all data]	0.0459
D_{calc}	1.619	*wR*2 [all data]	0.0599

Table S2 Selected Bond Distances (Å) in complex **1**

Dy1-O2	2.307(2)	Dy1-O3	2.336(2)	Dy1-O4a	2.443(2)
Dy1-O5	2.320(2)	Dy1-O6	2.346(2)	Dy1-O8	2.332(2)
Dy1-O9	2.329(2)	Dy1-O10	2.419(2)		

symmetry code: a = x, -y, z+1/2

Table S3 Hydrogen Bonds in **1**.

D-H	d(D-H) (Å)	<DHA(°)	d(D…A) (Å)	A
O10-H10A	0.933	168.38	2.818	O1 [x, y-1, z]
O10-H10B	0.922	163.94	2.855	O4 [-x, y, -z+3/2]
O11-H11A	0.989	151.29	2.815	O1 [-x, y, -z+3/2]

Table S4 Energies (cm^{-1}) of the calculated lowest Kramers doublets (KDs), *g* tensors of the Dy^{3+} fragments and the angels between g$_z$ of complex **1**.

KD		**1**		
		E, cm^{-1}	*g* tensor	
1	g_x	0.000	0.0506	0.0
	g_y		0.1099	
	g_z		19.3007	
2	g_x	104.012	1.0940	62.8
	g_y		2.0754	
	g_z		15.9993	
3	g_x	153.137	0.9596	37.4
	g_y		3.4912	
	g_z		10.9124	
4	g_x	215.619	3.0581	72.0
	g_y		5.1858	
	g_z		9.9057	
5	g_x	272.171	2.1714	80.3
	g_y		2.8892	
	g_z		11.5051	
6	g_x	326.977	0.64754	73.4
	g_y		0.97585	
	g_z		15.32606	
7	g_x	409.857	0.0881	94.4
	g_y		0.1538	
	g_z		17.5279	
8	g_x	473.876	0.0067	60.0
	g_y		0.0185	
	g_z		19.1100	

Table S5 Relaxation fitting parameters from Least-Squares Fitting of $\chi(f)$ data under zero and 1000 Oe dc field of **1**.

H_{dc} = 0 Oe				
T (K)	χ_T	χ_S	α	τ (s)
2	2.91	0.90	0.11	1.23E-5
4	1.43	0.33	0.078	1.10E-5
6	0.96	0.22	0.077	1.06E-5
8	0.71	0.17	0.073	1.07E-5
10	0.57	0.13	0.061	9.54E-6
11	0.52	0.083	0.092	7.69E-6
12	0.47	0.12	0.053	8.26E-6
13	0.43	0.10	0.047	6.68E-6
H_{dc} = 1000 Oe				
T (K)	χ_T	χ_S	α	τ (s)
7	0.89	0.012	0.11	0.00676
7.5	0.70	0.012	0.091	0.00323
8	0.60	0.011	0.076	0.00183
8.5	0.52	0.0095	0.073	0.00116
9	0.43	0.0089	0.062	7.22E-4
9.5	0.39	0.0080	0.062	4.89E-4
10	0.35	0.0075	0.061	3.29E-4
10.5	0.32	0.0055	0.085	2.37E-4
11	0.28	0.0070	0.056	1.64E-4
11.5	0.27	0.0048	0.083	1.17E-4
12	0.24	0.0033	0.11	8.37E-5
12.5	0.21	0.0048	0.092	5.89E-5
13	0.18	0.0012	0.15	3.96E-5
13.5	0.16	0.00085	0.14	2.85E-5
14	0.15	0.013	0.061	2.16E-5
14.5	0.14	0.0071	0.12	1.37E-5

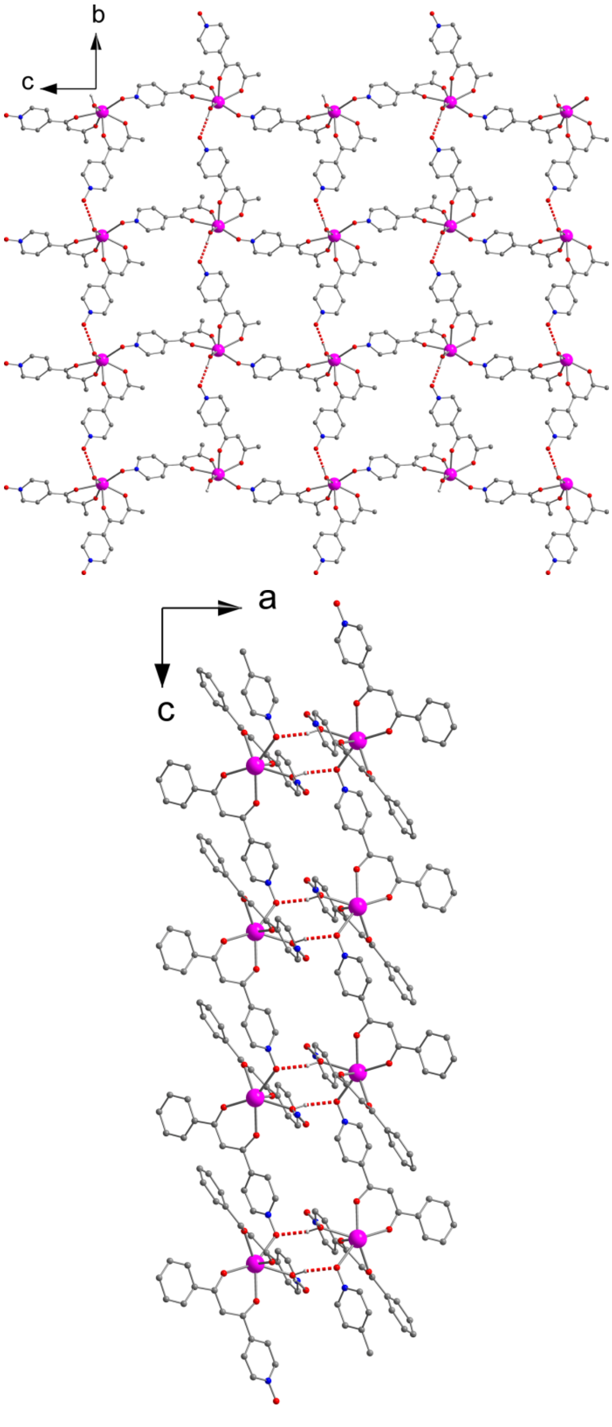

(b)

Fig. S1 The hydrogen-bonded 2D layer (a) and the connection of the hydrogen bonds between the layers (b) in **1**.

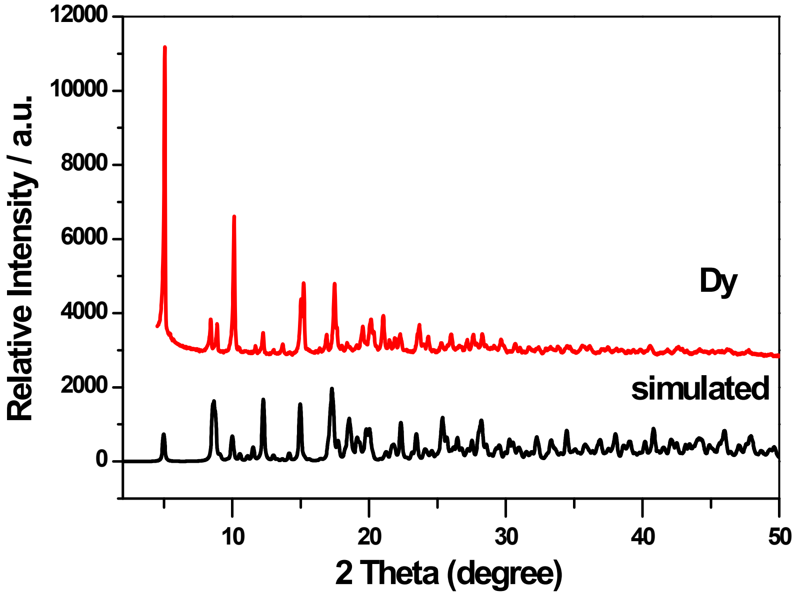

Fig. S2 Powder X-ray diffraction profiles of **1** together with a simulation from the single crystal data.

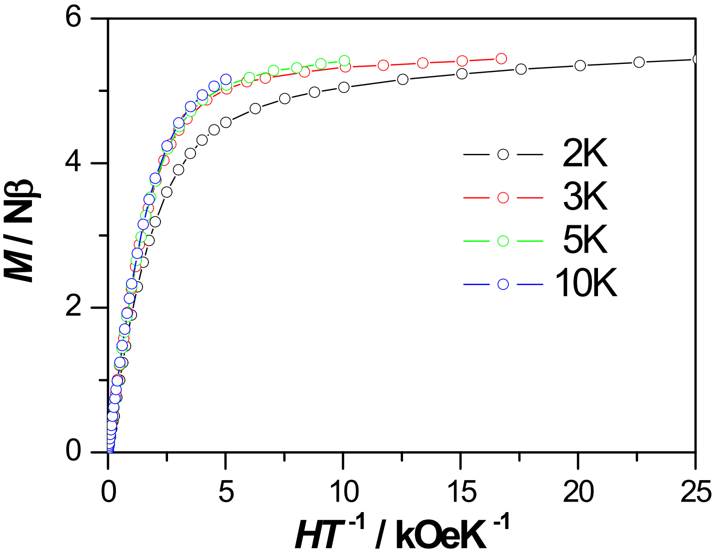

Fig. S3 Field dependence of the magnetization of **1** at different temperatures.

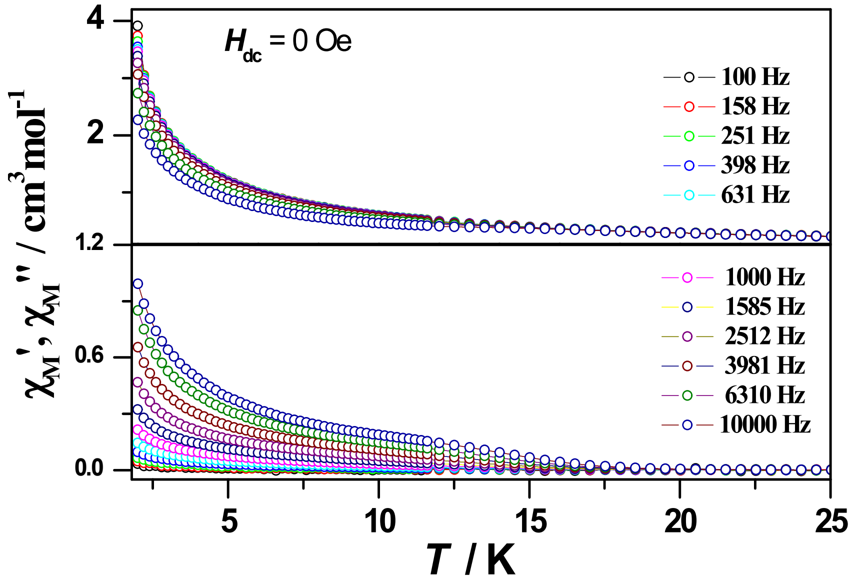

(a)

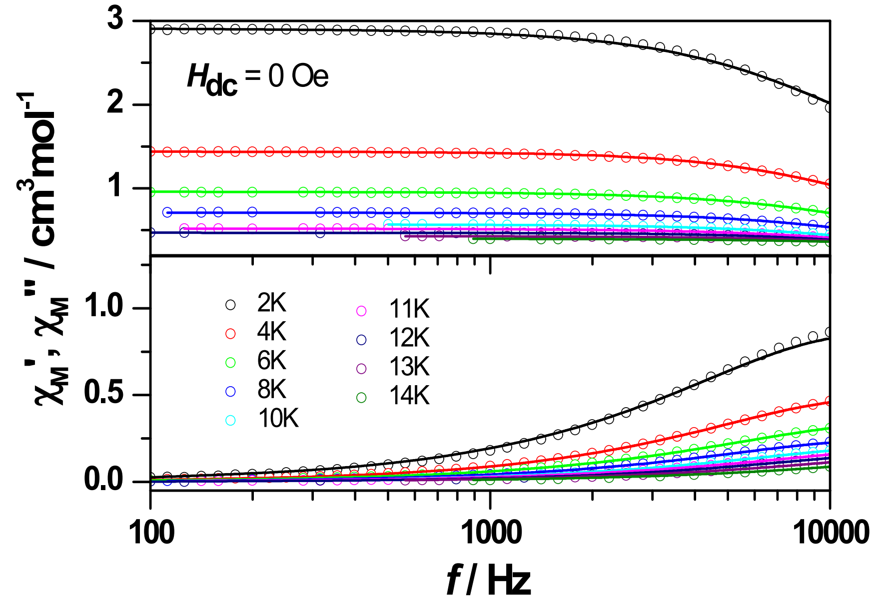

(b)

Fig. S4 Temperature dependence of the in phase χ_M' (top) and out-of-phase χ_M'' (bottom) ac susceptibility signals (a) and ac-f curves (b) under zero dc field the for **1**. Solid lines were fitted using a generalized Debye relaxation model, simultaneously to $\chi'(f)$ and $\chi''(f)$ curves.

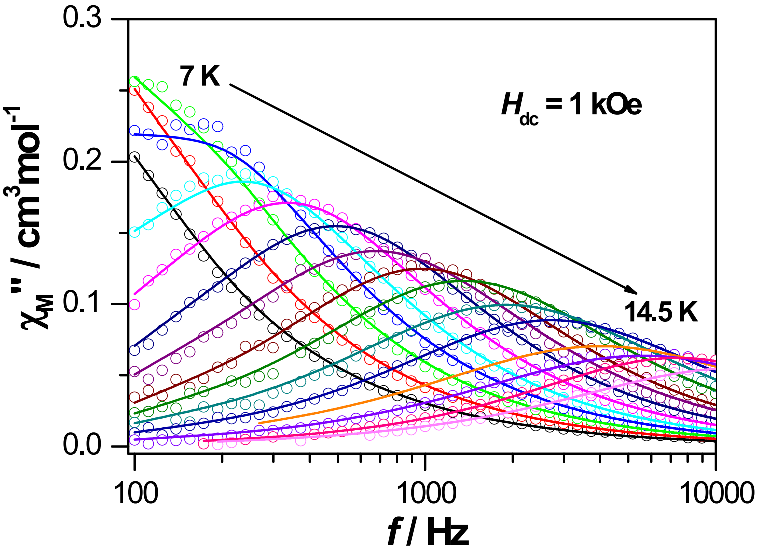

Fig. S5 *Ac-f* curves measured under 1 kOe dc fields for **1** at selected temperatures. Solid lines were fitted using a generalized Debye relaxation model, simultaneously to χ'' (*f*) curves.